

Label-Free Fluorescent Probing of G-Quadruplex Formation and Real-Time Monitoring of DNA Folding by a Quaternized Tetraphenylethene Salt with Aggregation-Induced Emission Characteristics

Yuning Hong,^[a] Matthias Häußler,^[a] Jacky W. Y. Lam,^[a] Zhen Li,^[a] King Keung Sin,^[a] Yongqiang Dong,^[a, b] Hui Tong,^[a] Jianzhao Liu,^[a] Anjun Qin,^[a, b] Reinhard Renneberg,^[a] and Ben Zhong Tang*^[a, b]

Abstract: Biosensing processes such as molecular beacons require non-trivial effort to covalently label or mark biomolecules. We report here a label-free DNA assay system with a simple dye with aggregation-induced emission (AIE) characteristics as the fluorescent bioprobe. 1,1,2,2-Tetrakis[4-(2-bromoethoxy)phenyl]ethene is nonemissive in solution but becomes highly emissive when aggregated. This AIE effect is caused by restriction of intramolecular rotation, as verified by a large increase in the emission intensity by increasing viscosity and decreasing temperature of the aqueous buffer solution of 1,1,2,2-tetrakis[4-(2-triethyl-

ammonioethoxy)phenyl]ethene tetra-bromide (TTAPE). When TTAPE is bound to a guanine-rich DNA strand (G1) via electrostatic attraction, its intramolecular rotation is restricted and its emission is turned on. When a competitive cation is added to the G1 solution, TTAPE is detached and its emission is turned off. TTAPE works as a sensitive poststaining agent for poly-(acrylamide) gel electrophoresis (PAGE) visualization of G1. The dye is

highly affinitive to a secondary structure of G1 called the G-quadruplex. The bathochromic shift involved in the G1 folding process allows spectral discrimination of the G-quadruplex from other DNA structures. The strong affinity of TTAPE dye to the G-quadruplex structure is associated with a geometric fit aided by the electrostatic attraction. The distinct AIE feature of TTAPE enables real-time monitoring of folding process of G1 in the absence of any pre-attached fluorogenic labels on the DNA strand. TTAPE can be used as a K⁺ ion biosensor because of its specificity to K⁺-induced and -stabilized quadruplex structure.

Keywords: biosensors • DNA • dyes • fluorescent probes • G-quadruplex

Introduction

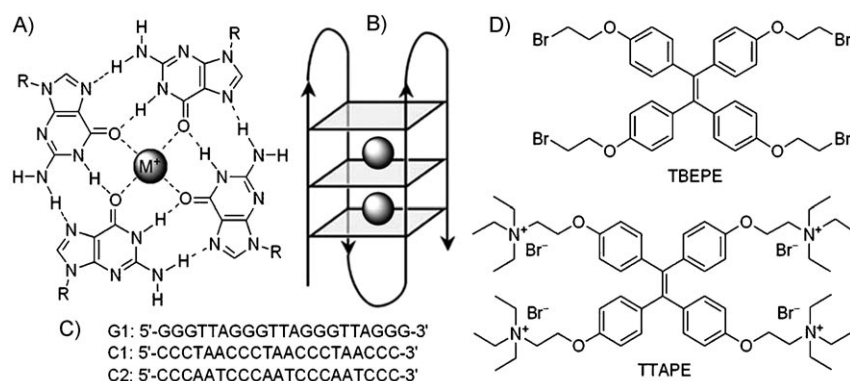
A single-stranded (ss) DNA with guanine (G)-rich repeat sequences can assume a square-planar arrangement of the G units stabilized by Hoogsteen hydrogen bonds (Scheme 1 A).

An array of these G-quartets can stack on top of each other to form a secondary structure called a G-quadruplex (Scheme 1 B). This structure is further stabilized by the monovalent cations (e.g., K⁺) located in the centers of G-tetrads.^[1–3] It is predicted that thousands of DNA sequences sprinkled over the human genome are potential quadruplex-forming sites, making the tetrad structure one of the most prevalent regulatory motifs in the body.^[4] Much effort has been devoted to the studies on the biology of genomic and telomeric G-quadruplexes.^[5] It has been found, for example, that quadruplex formation can affect gene expression and inhibit telomerase activity in cancer cells.^[6,7] It has been envisioned that quadruplex-targeting drugs may enable artificial regulation of gene expression and control of cancer-cell proliferation. Clearly, efficient probing of G-quadruplex structures is a prerequisite to the rational design of quartet-specific medication and telomere-aimed anticancer therapy.^[8]

[a] Y. Hong, Dr. M. Häußler, Dr. J. W. Y. Lam, Dr. Z. Li, Dr. K. K. Sin, Dr. Y. Dong, Dr. H. Tong, J. Liu, Dr. A. Qin, Prof. Dr. R. Renneberg, Prof. Dr. B. Z. Tang
Department of Chemistry
The Hong Kong University of Science & Technology
Clear Water Bay, Kowloon, Hong Kong (China)
Fax: (+852)2358-1594
E-mail: tangbenz@ust.hk

[b] Dr. Y. Dong, Dr. A. Qin, Prof. Dr. B. Z. Tang
Department of Polymer Science and Engineering
Zhejiang University, Hangzhou 310027 (China)

Supporting information for this article is available on the WWW under <http://www.chemurj.org/> or from the author.



Scheme 1. A) Structure of a G-quartet showing the hydrogen bonds between G units and the interaction with a cation (M^+). B) Sketch of a G-quadruplex folded by a human telomeric DNA strand. C) Sequences of G1 and its complementary (C1) and non-complementary (C2) strands. D) Structures of the fluorogenic dyes investigated in this work: 1,1,2,2-tetrakis[4-(2-bromoethoxy)phenyl]ethene (TBEPE) and 1,1,2,2-tetrakis[4-(2-triethylammonioethoxy)phenyl]ethene tetrabromide (TTAPE).

A variety of techniques, including NMR spectroscopy, mass spectrometry, circular dichroism (CD), UV melting profile analysis, poly(acrylamide) gel electrophoresis (PAGE), and surface plasmon resonance, have been used to study G-quadruplex formation.^[8,9] These methods, however, require large quantities of DNA samples because of their poor sensitivities. Fluorescence (FL)-based probe systems, on the other hand, offers superb sensitivity, low background noise, and a wide dynamic working range.^[10] A few FL sensors based on “molecular beacons” and fluorescent resonant energy transfer processes have been developed, which prove to be powerful in studying conformational transitions of quadruplexes.^[11] These processes, however, require prelabeling of oligonucleotides by fluorophores or dual tagging on a single DNA strand by chemical reactions. Precise synthesis of a DNA–dye conjugate is a nontrivial job and product isolation and purification is often painstaking. Furthermore, structural changes caused by the chemical modifications may affect conformations of the G-quadruplexes and interfere with their folding kinetics.^[12]

Biological processes occur in physiological fluids and accordingly, biological assays are commonly conducted in aqueous buffer solutions. The working units in the FL probes, however, are hydrophobic aromatic rings and other π -conjugated chromophores. The FL dyes tend to aggregate when absorbed onto strand surfaces or after entering hydrophobic pockets of folded strands owing to the incompatibility of the dyes with the hydrophilic media and the π – π stacking interaction between their π -conjugated chromophores. The aggregate formation normally quenches light emissions of the dyes, which poses a thorny obstacle to the development of efficient FL probes.^[9b,13] Various approaches have been taken in an effort to impede aggregate formation, such as using long spacers to separate chromophoric units.^[13] Obviously, it is nicer and more desirable to have sensitive and selective G-quadruplex probes that do not require premodifications of the DNA strands and that do not suffer from aggregation-caused emission quenching.

We and others have recently observed a novel phenomenon of aggregation-induced emission (AIE): a series of nonemissive dyes, such as siloles, butadienes, pyrans, fulvenes, biaryls, and tetraphenylethenes (TPE), are induced to luminesce by aggregate formation.^[14–16] The AIE dyes are not only excellent emitters for the fabrication of efficient light-emitting diodes but also sensitive probes for the detection of biomolecules.^[14–17] Among them, the TPE-based dyes have received much attention because of their facile synthesis, ready functionalization, good photostability, and high

FL quantum yields (Φ_F).^[15] In this work, we synthesized a new AIE-active TPE salt, that is, 1,1,2,2-tetrakis[4-(2-triethylammonioethoxy)phenyl]ethene tetrabromide (TTAPE), and explored its potential application as a G-quadruplex probe by using an oligonucleotide of 5'-GGGTTAGGGTTAGGGTTAGGG-3' or $[dG_3(T_2AG_3)_3]$ (G1) as a model DNA molecule that mimics the T_2AG_3 repeat sequences in the single-stranded region of a human telomere (Scheme 1). In an aqueous buffer solution, the nonemissive TTAPE dye becomes highly luminescent upon its binding to G1 via electrostatic attraction owing to its multiple positive charges. When G1 folds into a G-quadruplex structure, the emission peak (λ_{em}) of the AIE dye undergoes a noticeable bathochromic shift, allowing easy differentiation of the G-quadruplex from other DNA structures. The folding processes of G1 can be followed by the time-dependent FL measurement of the AIE dye.

Results and Discussion

Dye synthesis: TTAPE was prepared by the synthetic route shown in Scheme S1 in the Supporting Information. Dehydrobromination of 4,4'-dihydroxybenzophenone (DHBP) with 1,2-dibromoethane in the presence of potassium carbonate yields 4,4'-bis(2-bromoethoxy)benzophenone (BBEBP). McMurry coupling^[18] of BBEBP produces 1,1,2,2-tetrakis[4-(2-bromoethoxy)phenyl]ethene (TBEPE), which is quaternized by triethylamine to furnish a salt 1,1,2,2-tetrakis[4-(2-triethylammonioethoxy)phenyl]ethene tetrabromide (TTAPE). The reaction intermediates and final product were fully characterized by spectroscopic methods from which satisfactory analysis data were obtained (see Figure S1 and the characterization data in the Supporting Information). TBEPE is completely soluble in chloroform, acetonitrile (AN), and THF, slightly soluble in ethanol and methanol, but totally insoluble in water. TTAPE, on the other hand, is soluble in water as well as all the organic sol-

vents mentioned above owing to the amphiphilic nature of the ammonium salt.

AIE effect: When dissolved in good solvents, TBEPE is virtually nonluminescent at the molecular level. The addition of poor solvents into solutions of TBEPE dramatically boosts its emission efficiency. A dilute AN solution of TBEPE, for example, emits a faint UV light (see Figure S2 in the Supporting Information). When a large amount of water (99 vol %) is added, the resultant mixture shows an intense FL spectrum with a peak at 479 nm. As water is a poor solvent of TBEPE, its molecules aggregated in the aqueous mixture. TBEPE is therefore induced to emit light by aggregate formation; in other words, it is AIE active. The mixture is transparent and homogeneous, suggesting that the dye aggregates suspended in the mixture are nano-sized. In the dilute AN solution, the phenyl rings of TBEPE can rotate against its central olefinic double bond, which nonradiatively deactivates the excited state and renders the dye nonemissive. The intramolecular rotations are largely restricted in the nanoaggregates in the AN/water mixture. This blocks the nonradiative decay channel of the dye and makes it highly luminescent.^[15]

Changes in the Φ_F values of TBEPE in the AN/water mixtures with different water contents further confirm its AIE nature. In the AN solution, TBEPE exhibits a negligibly small Φ_F value ($\approx 0.5\%$), which remains almost unchanged until up to approximately 60% of water is added (Figure 1A). Afterwards, the Φ_F value starts to increase swiftly. In the AN/water mixtures with lower water fractions, TBEPE is genuinely dissolved, whereas in the aqueous mixtures with higher water fractions ($> 60\%$), the dye molecules cluster together owing to the deterioration of the solvation power of the mixture. When the water fraction is increased to 99 vol %, the Φ_F value is increased to approximately 18%, which is approximately 35-fold higher than that in the pure AN solvent. The absolute Φ_F values of the aggregates should be much higher than the relative ones

given in Figure 1A, if the light scattering caused by the Mie effect of the nanoaggregates is taken into consideration.^[19]

TTAPE is completely soluble in water. Owing to its amphiphilic nature associated with its quaternary tetraalkylammonium moieties, addition of AN, THF, or methanol to the solution of the sample in water fails to make the dye molecules aggregate. As a result, the emissions from TTAPE in all these mixtures are as weak as that in the pure water solution. However, increasing viscosity and decreasing temperature of the solution of TTAPE can activate its FL process. As can be seen from Figure 1B, TTAPE in a viscous glycerol/water mixture at 25 °C emits an intense blue light of 464 nm. When the viscous mixture is cooled to -78 °C , its emission intensity is further increased. At the cryogenic temperature, solvent viscosity is increased and molecular motions are further hampered. TTAPE can thus be induced to emit light by restricting its intramolecular rotations, which is the exact cause for the AIE effect of its TBEPE cousin (see earlier).^[15,20]

DNA probing: G1 is a 21-mer ssDNA molecule that mimics the human telomeric sequence. When the DNA molecules are added into a solution of TTAPE in a tris(hydroxymethyl)aminomethane (Tris)-HCl buffer solution, the solution starts to luminesce (Figure 2A). Similar FL “light up” phenomenon has been observed in the thiazole orange system.^[21] The I/I_0 ratio of TTAPE at 470 nm increases rapidly in a narrow DNA concentration range and reaches its maximum at $[G1] \approx 5\ \mu\text{M}$ (Figure 2B). Although conventional FL dyes suffer from a self-quenching problem at high dye concentrations,^[22] the FL of TTAPE is continuously intensified with increasing concentration (see Figure S3 in the Supporting Information and Figure 2B) owing to its unique AIE feature. In the aqueous buffer solution, the cationic dye spontaneously binds to the anionic DNA molecule through electrostatic attraction, resulting in the formation of a TTAPE/G1 complex. Hydrophobic interaction between TTAPE and G1 may have also played a role in the binding process. These intermolecular forces lock conformations of the TTAPE molecules bound to the G1 strands. Consequently, the intramolecular rotations of TTAPE are restricted, which thus blocks its radiationless relaxation pathways and activates its FL process.

The FL “turn-on” switching of TTAPE by binding to the G1 strand inspired us to check whether it can be used as a DNA marker in the PAGE assay. After running PAGE of G1 in a Tris-borate-ethylene-diaminetetraacetic acid (TBE) buffer solution, the gel is stained by a TTAPE solution

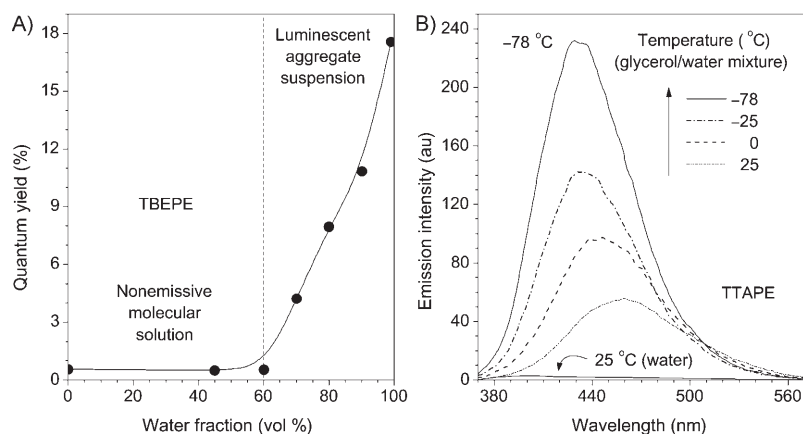


Figure 1. A) Plot of quantum yield of TBEPE versus composition of the AN/water mixture. B) FL spectra of TTAPE in a glycerol/water mixture (99:1 by volume) at different temperatures; the spectrum of its water solution at 25 °C is shown for comparison. $[\text{dye}] = 5\ \mu\text{M}$; $\lambda_{\text{ex}} = 350\ \text{nm}$.

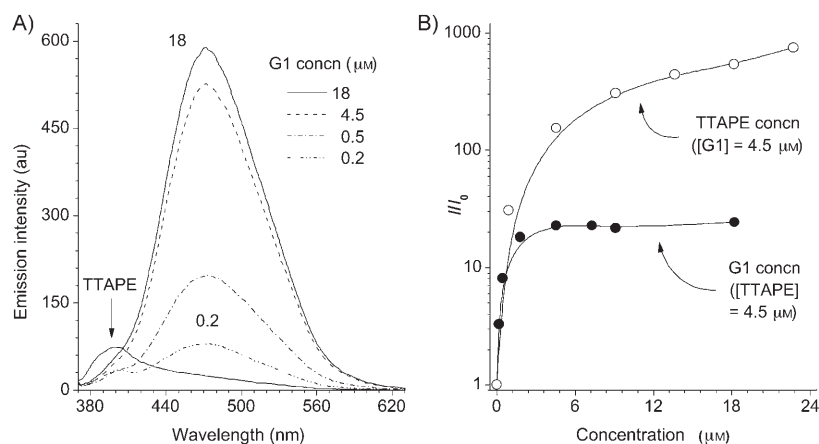


Figure 2. A) Fluorimetric titration of G1 to an aqueous solution of TTape (4.5 μM) in 5 mM Tris-HCl buffer solution (pH 7.50). B) Change in emission intensity (I) at 470 nm with variation in concentration of G1 or TTape; $\lambda_{\text{ex}} = 350$ nm.

for 5 min. Upon UV illumination, the stained gel shows FL bands at various G1 concentrations (Figure 3A). Ethidium bromide (EB) is a widely used visualization agent for PAGE

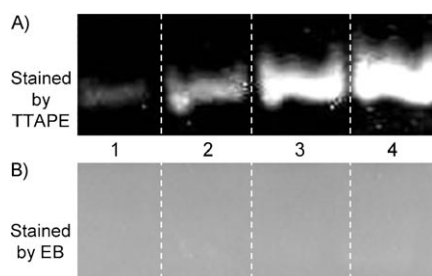


Figure 3. PAGE assays of G1 at concentrations of 0.5, 1.0, 5.0, and 10.0 μM (lanes 1–4). The gels were poststained by 10 μM TTape (A) and 1.3 μM EB (B) for 5 min.

assays.^[23] The gel stained by EB exhibits bright background emissions (Figure 3B), although a much lower EB concentration has been used. The G1 bands are not visualized until the gel has been stained by EB for as long as 30 min. Band visualization by EB is usually realized by its intercalation into the hydrophobic region of DNA, which makes the staining a slow process. On the other hand, the FL of TTape is activated by its spontaneous electrostatic interaction with the charged surface of DNA, which can be achieved in a short time. Sensitivity tests reveal that TTape can detect approximately 0.5 μM of G1. The detection limit can be further lowered by increasing the dye concentration, as suggested by the solution I/I_0 data (see Figure 2B). Our system thus has the advantages of fast response and high sensitivity in addition to its excellent miscibility with aqueous media.

Quadruplex recognition: In the aqueous buffer solution, G1 takes a random coil conformation and shows a weak CD

curve (Figure 4). Adding K^+ ions into the G1 solution (G1/ K^+) promotes formation of the G quadruplex,^[24] which brings about a change in the CD spectral profile as well as an increase in the ellipticity. The G1/TTape/ K^+ system shows a CD curve with a similar profile and ellipticity, implying that the dye does not affect the quadruplex conformation. The quadruplex formation induces an approximate 20 nm red-shift in both excitation and emission spectra of TTape (Figure 5). A serial titration experiment with K^+

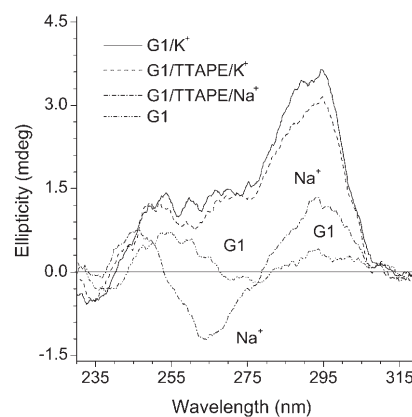


Figure 4. CD spectra of G1 in a Tris-HCl buffer solution in the presence or absence of a metal ion and/or TTape at 20°C. $[\text{G1}] = 9 \mu\text{M}$, $[\text{ion}] = 0.5 \text{ M}$, $[\text{TTape}] = 4.5 \mu\text{M}$.

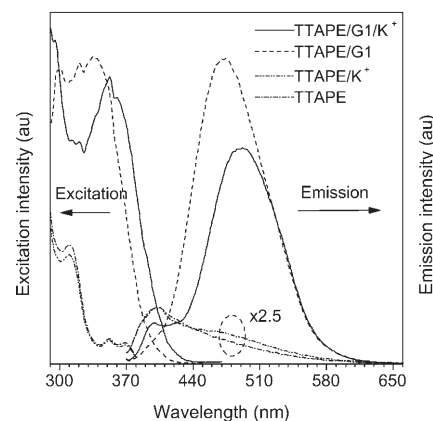


Figure 5. Excitation and emission spectra of TTape solutions in a Tris-HCl buffer solution in the presence or absence of K^+ ion and/or G1. $[\text{TTape}] = 4.5 \mu\text{M}$, $[\text{G1}] = 9 \mu\text{M}$, $[\text{K}^+] = 0.5 \text{ M}$; $\lambda_{\text{ex}} = 350$ nm.

ions as titrate reveals that the spectral red-shift starts from $[\text{K}^+] \approx 10 \text{ mM}$ and completes at $[\text{K}^+] \approx 100 \text{ mM}$ (see Figure S5 in the Supporting Information). The FL intensity at

470 nm, on the other hand, is monotonically decreased with increasing the K^+ ion concentration. Closer inspection of the data finds that the spectrum at high $[K^+]$ contains a shoulder band at approximately 400 nm. This shoulder is probably associated with the emission of the TTape molecules that are still bound to the quadruplex but through only one or two of its four ammonium arms. These partially bound dye molecules may undergo partial intramolecular rotations and thus emit weak light in the blue spectral region.

The addition sequence is systematically investigated to see how it affects the FL and CD spectra of the TTape/quadruplex structure. As can be seen from the data summarized in Table 1 and Figure S6 in the Supporting Information, the

Table 1. Effect of addition sequence on FL and CD intensities of TTape/quadruplex complexes at room temperature.^[a]

Entry	Mixture ^[b]	Additive	FL intensity ^[c]	CD intensity ^[d]
1 ^[e]	TTape/G1	K^+	1.00	1.00
2	TTape/ K^+	G1	0.82	0.92
3	G1/ K^+	TTape	0.70	0.88

[a] For comparison, final concentrations of the three components in all the mixtures were adjusted to be the same. [b] Incubated at 4 °C for 30 min. [c] Relative intensity at 492 nm. [d] Relative intensity at 295 nm. [e] Data corresponding to those given in Figure 4 and Figure 5.

FL/CD intensities vary in the order of the following addition sequence: $K^+ \rightarrow \text{TTape/G1} > \text{G1/K}^+ \rightarrow \text{TTape/K}^+ > \text{TTape} \rightarrow \text{G1/K}^+$. Comparison of the data in Table 1, entries 1 and 2 suggests that some TTape molecules pre-bound to the G1 strands have been incorporated into the G-quadruplex structure during the K^+ -induced structural transformation. When TTape is added after the G-quadruplex has been formed (Table 1, entry 3), the dye molecules are difficult to bind to the quadruplex surrounded by numerous K^+ ions, hence the observed lowest FL and CD intensities. The profiles of the CD spectra for all the G-quadruplexes formed in the three entries are almost identical (see Figure S6B in the Supporting Information), confirming that TTape does not appreciably distort the G-quadruplex structure.

Effects of cationic species: As stated above, addition of K^+ ions into TTape/G1 results in a quadruplex-specific emission peak at 492 nm. Addition of Na^+ ions into TTape/G1, however, quenches this band (Figure 6A, inset). Similarly, other cationic species including Li^+ , NH_4^+ , Mg^{2+} , and Ca^{2+}

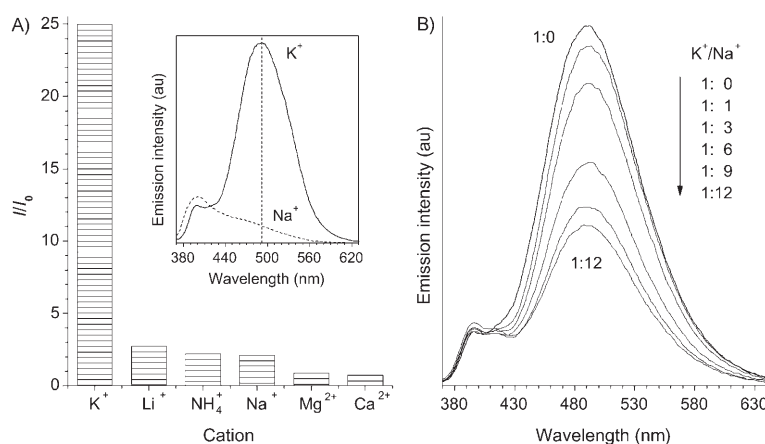


Figure 6. A) Dependence of FL intensity of TTape at 492 nm on cationic species ($[ion] = 500 \text{ mM}$). Inset: FL spectra of TTape in the buffer solutions containing G1 and K^+ or Na^+ ion. B) Variation in the FL spectrum of TTape/G1/ K^+ solution with the addition of Na^+ ions. $[TTape] = 4.5 \text{ }\mu\text{M}$, $[G1] = 9 \text{ }\mu\text{M}$, $[K^+] = 100 \text{ mM}$; $\lambda_{ex} = 350 \text{ nm}$.

all attenuate this emission band (see Figure S7 in the Supporting Information). After the addition into TTape/G1, these cationic species compete with TTape for binding with G1. The externally added cationic species prevails because its amount is greater than 10^4 -fold higher than that of TTape. Once the dye molecules are stripped from the DNA strand, their intramolecular rotations are no longer restricted and the AIE band is thus turned off. The FL spectrum of TTape/G1 in the presence of K^+ is clearly different from, and its peak intensity is outstandingly higher than, those in the presence of other cations. This suggests the potential utility of TTape/G1 as a K^+ ion biosensor.

Among the cationic species, Na^+ and NH_4^+ ions are known to be able to induce quadruplex formation,^[1,25] but the TTape emission is still diminished by these cations. It is known that the conformation of G-quadruplex is highly dependent on the type of cationic species. In the presence of Na^+ ions, G1 exhibits a CD spectrum with positively and negatively signed Cotton effects at 295 and 265 nm, respectively (see Figure 4). This suggests the formation of a G-quadruplex with an antiparallel strand alignment, which differs from the G-quadruplex with a mixed parallel/antiparallel strand arrangements formed in the presence of K^+ ions.^[24,26] The difference in the geometric conformation may account for the observed difference in the emission behavior. This offers an attractive possibility of using TTape as a bioprobe to discriminate between quadruplexes with different conformations.

Various electrolytes exist in the biological systems and excess or absence of one or two of these ionic species can cause biomolecules to undergo conformational transitions, resulting in either favorable biological effects or undesirable dysfunctions. How does the coexistence of two cationic species, for example, physiologically important K^+ and Na^+ ions, affect the quadruplex conformation? As can be seen from Figure 6B, the addition of Na^+ ions into TTape/G1/ K^+ gradually decreases the intensity of the quadruplex-spe-

cific emission at 492 nm. The large amount of Na^+ ions drives the dye molecules chemisorbed on the G-quadruplex surface into the aqueous media, resulting in the observed emission attenuation. The spectral profile, however, remains unchanged, even when the amount of the added Na^+ ions is 12-fold higher than that of K^+ ions, indicating that the G-quadruplex has maintained its structural integrity. This is further proved by the CD data: the CD spectrum of the G-quadruplex formed in the presence of K^+ ions is unaffected by the perturbations from the excess amount of externally added Na^+ ions (see Figure S8 in the Supporting Information). This suggests that the K^+ -containing quadruplex is more stable than the Na^+ ion quadruplex or that the K^+ ion is superior to the Na^+ ion in inducing/stabilizing the quadruplex structure.^[25]

It is clear that TTape has a high affinity for the K^+ -containing G-quadruplex but not its Na^+ ion cousin. Isothermal titration calorimetry (ITC) measurements are performed, in an effort to understand the thermodynamic basis for the binding affinity difference. ITC is a sensitive technique for the studies of bimolecular processes and can provide direct information about binding affinities and associated thermo-

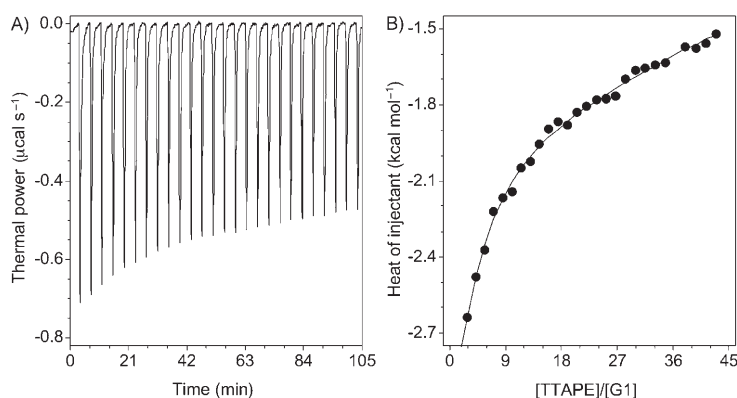


Figure 7. A) Calorimetric curves for titration of G1 in a K-Tris buffer solution with serial injections of TTape at 25 °C. B) Binding isotherm as a function of [TTape]/[G1] molar ratio in the buffer solution.

dynamic parameters.^[27] As can be seen from Figure 7A, injection of a tiny aliquot (10 μL) of a TTape solution into a G1/ K^+ buffer solution yields a large exothermic peak. Fitting the data of integrated heat generated per injection in the binding isotherm (Figure 7B) gives a binding constant (K_b) of $2.4 \times 10^5 \text{ M}^{-1}$, from which a Gibbs energy (ΔG°) of $-7.3 \text{ kcal mol}^{-1}$ is obtained. However, in the case of the Na^+ ion titration, the binding constant is too small to be determined accurately from the ITC data.

Effects of DNA strands: If a DNA contains no G unit, its TTape complex ceases to show the quadruplex-specific response to K^+ ions. C1 is also a 21-mer ssDNA, but unlike G1, it possesses no G-rich repeat sequence. When C1 is admixed with TTape, a blue emission at 474 nm results (see Figure S9A in the Supporting Information). This emission

is, however, quenched upon addition of other cations including K^+ ions. Different from G1, C1 cannot fold into a G-quadruplex structure in the presence of K^+ ions. The K^+ ions here just compete with the TTape molecules for DNA binding, thus resulting in the expulsion of the dye molecules from the C1 strand and the quenching of the light emission.

To be qualified as a specific probe for G-quadruplex recognition, the dye must be able to distinguish the quadruplex from other DNA conformations, especially the double-stranded (ds) conformation, which is the most ubiquitous conformation for DNA molecules in living organisms.^[28] C1 is a complementary strand of G1: the two DNA strands hybridize to form a duplex (see Figure S10 in the Supporting Information). The dsDNA molecules induce TTape to emit at 470 nm, which is different from the dye emission in

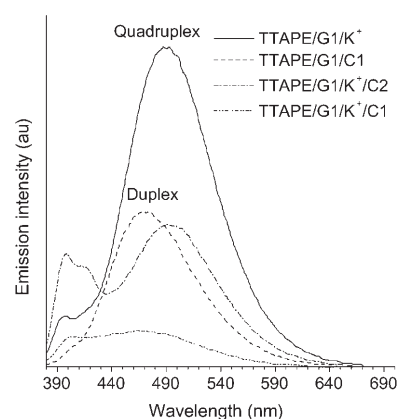


Figure 8. Emission spectra of TTape/G1 in a Tris-HCl buffer solution in the presence of K^+ and/or C1 or C2. [TTape] = 4.5 μM, [K^+] = 0.5 M; λ_{ex} = 350 nm; [G1] = 9 μM (in the absence of C_i), [G1] = [C_i] = 4.5 μM (in the presence of C_i).

the presence of the G-quadruplex (λ_{em} = 492 nm; Figure 8). The interaction of TTape with dsDNA molecules is again electrostatic in nature: when large amounts of other cations are added into G1/C1 solutions, the bound dye molecules are replaced by the externally added cations and the AIE emission band is accordingly attenuated (see Figure S11B in the Supporting Information).

For comparison, the quadruplex/TTape complex is mixed with equal molar amounts of its complementary and noncomplementary strands C1 and C2, respectively. The resultant TTape/G1/ K^+ /C_i mixtures (where *i* represents either 1 or 2) are annealed at approximately 58 °C, which is a temperature approximately 2 °C below the melting points of the DNA molecules (≈ 60 °C). The hybridization of G1 with C1 unfolds the G-quadruplex structure and yields a duplex (dsDNA). As a result, the quadruplex-specific emission at 492 nm is quenched (Figure 8). The duplex is saturated by the prevalently large amount of K^+ ions and leaves little room for TTape molecules to bind, hence making the solution nonemissive. Similar results are obtained for other cationic species (see Figure S9B in the Supporting Information).

As C2 is noncomplementary to G1, the G-quadruplex remains unperturbed and the emission at 492 nm is preserved. Intriguingly, however, the emission in the bluer region (at ≈ 400 nm) is increased upon admixing with C2. Although the whole strand of C2 is noncomplementary to G1, partial hybridization of some base units of C2 with those of the G-quadruplex of G1, especially those on its surface, through GC and/or AT base pairing is possible. Such pairing replaces some, although not all, of the ammonium groups of a TTAPE bound to the G-quadruplex. The dye molecules hanging on the quadruplex through one or two ammonium arms can undergo partial intramolecular rotations and thus emit in the bluer spectral region. Addition of large amounts of other cationic species into the TTAPE/G1/C2 solutions drives all the dye molecules out of touch with the DNA strands. As a result, the solutions become nonemissive (see Figure S11 in the Supporting Information).

Time-dependent FL: To gain insight into the dynamics of the folding process of G1, time-dependent FL measurements are performed. Solutions containing TTAPE and G1 are first incubated for 30 min to ensure complete dye/DNA complexation. A solution of potassium chloride is then injected at time $t=0$ (automatic injection mode) and the emission intensity at 470 nm is monitored. The emission drops abruptly to approximately 30% of its original intensity at the beginning but starts to recover after approximately 8 s and finally reaches a plateau at approximately 320 s (Figure 9). This suggests a very fast ion-exchange process

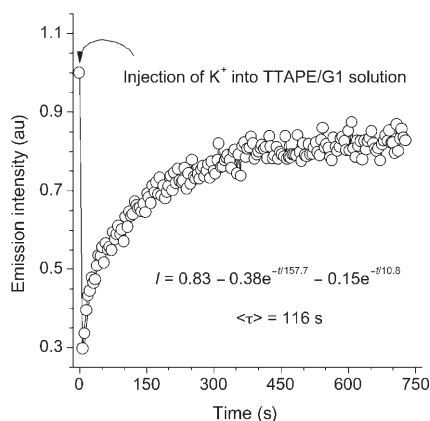


Figure 9. Time course of evolution of emission intensity at 470 nm of TTAPE/G1 in a Tris-HCl buffer solution after injection of a K^+ solution. $[\text{TTAPE}] = 4.5 \mu\text{M}$, $[\text{G1}] = 9 \mu\text{M}$, $[\text{K}^+] = 0.5\text{M}$; $\lambda_{\text{ex}} = 350\text{ nm}$.

between K^+ ions and TTAPE with G1 at the beginning. Because of its smaller size and higher concentration, K^+ outperforms TTAPE in the DNA binding, leading to the initial quick drop in the FL intensity. The G1 strand then starts to fold into the quadruplex with the aid of K^+ ions during which the TTAPE molecules are attracted to bind with the quadruplex, as is manifested by the recovery of the FL signal after approximately 8 s. The complete folding of G1

into the quadruplex conformation takes only approximately 5 min. This result is consistent with the observations in the previous studies on the DNA folding processes by using the surface plasmon resonance and electrospray mass spectrometry techniques.^[9d,25b]

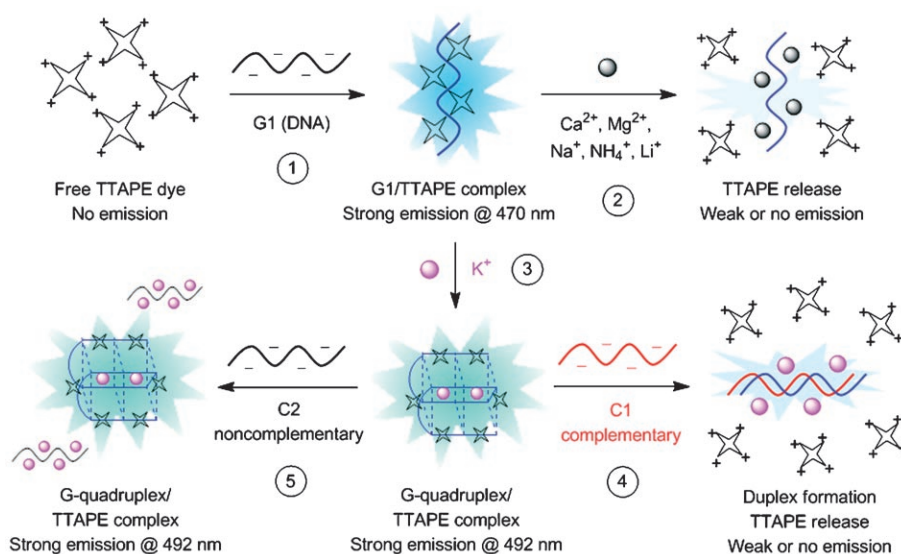
The FL recovery process can be fitted by a double-exponential curve, giving a weighted mean time constant ($\langle \tau \rangle$) of 116 s. The inverse of $\langle \tau \rangle$ can be viewed as a rate constant, allowing one to have a kinetic picture of the folding process of the DNA.^[29] Control experiments with other cationic species such as Na^+ , NH_4^+ , and Ca^{2+} ions reveal similar FL decreases (see Figure S12 in the Supporting Information), suggesting that the same ion-exchange mechanism is involved in the dye detachment processes. The emission intensities, however, fail to recover from the low values even after a time period as long as 1000 s. For Na^+ and NH_4^+ ions, it is probably caused by the geometric unfit of TTAPE with the G-quadruplexes formed in the presence of these two cationic species. For Ca^{2+} ions, it is simply because this ion cannot induce the formation of a G-quadruplex structure.

Binding interactions: All experimental results indicate that TTAPE has a high affinity to the quadruplex structure over other DNA structures and that its interaction with the quadruplex is mainly electrostatic in nature. However, the unusually high resistance of the G-quadruplex/TTAPE complex to other competing cations suggests that other forces may also participate in the binding processes. NMR spectroscopy (solution) and X-ray diffraction (crystal) analyses of G-quadruplex structures reveal distinct geometric features associated with different parallel and antiparallel strand alignments as well as their mixed modes of arrangements.^[30] These G-quadruplex structures offer several binding sites, that is, two planar end surfaces, four grooves, a channel of negative electrostatic potential, and flexible-loop regions.^[31] The strong binding of the dye molecules to the G-quadruplex may be attributed to a nice geometric fit. Careful examination of the crystal structure of human telomeric sequence of $\text{d}[\text{AG}_3(\text{T}_2\text{AG}_3)_3]$ (protein data bank No. 1 KF1) reveals a resemblance of the G-quartet to a square aromatic plane with a width of 10.9 Å and a diagonal length of 13.6 Å (see Figure S13 in the Supporting Information). This dimensional size is slightly larger than that of the TPE core of TTAPE, which allows the core to dock on the G-quartet of the quadruplex. The docking or stacking of the dye molecules on the surfaces of the end G-quartets forces the twisted phenyl rings to take more coplanar conformations, hence the observed characteristic red-shift in the FL spectrum. The multiple cationic ammonium arms may interact with the quadruplex grooves, further strengthening the dye association.

The aromatic planes of TTAPE may also stack on the grooves through hydrophobic contact with the ammonium arms by insertion into the holes that are formed by two adjacent phosphate dipoles of the TTA loops. The TPE core of TTAPE may be compelled to assume a more planar conformation to accommodate a better geometric fit. As the

groove dimension varies with the different type of G-quadruplex, the groove binding offers the opportunity for selective bioprobings that can discriminate between quadruplex conformations with different strand alignments. The selectivity of the K^+ -driven quadruplex over the Na^+ ion quadruplex is probably an example of this type of conformation-based biodiscrimination.

Biosensing processes: It has now become clear that TTAPE is a fluorescent marker that can perform multiple functions, including DNA probing, G-quadruplex recognition, and potassium-ion sensing (Scheme 2). The nonemissive TTAPE



Scheme 2. Fluorescent bioprobings processes of TTAPE.

molecules dissolved in the aqueous buffer solution become highly luminescent upon binding to G1 through primarily electrostatic attraction as the DNA binding restricts their intramolecular rotations (process 1). Addition of competitive cations such as Li^+ , Na^+ , NH_4^+ , Mg^{2+} , and Ca^{2+} ion weakens or quenches the emission because the cations drive the bound dye molecules back into solution (process 2). Addition of K^+ ions, however, induce G1 to fold into a G-quadruplex structure, resulting in a redshift in the emission spectrum (process 3). Hybridization with a complementary ssDNA (C1) unfolds the G quadruplex and affords a duplex. The K^+ ions in the solution compete with the TTAPE molecules for binding with the dsDNA. The dye molecules are released back to the solution and the emission is thus diminished (process 4). On the other hand, a noncomplementary ssDNA strand (C2) does not disassemble the G-quadruplex structure. As a result, the characteristic emission of the quadruplex/TTAPE complex at 492 nm is preserved (process 5).

Conclusion

In this work, we have successfully synthesized a water-soluble TPE derivative, that is, TTAPE, with novel AIE characteristics. We have shown that TTAPE can function as a “light-up” bioprobe for DNA detection, G-quadruplex identification, and potassium-ion sensing. We have demonstrated that TTAPE can be utilized as an external fluorescent marker to study conformational structures, to monitor folding processes of label-free oligonucleotides with G-rich strand sequences, and to visualize DNA bands in PAGE assays. The spectral redshift diagnostically signals the presence of quadruplex structure,

allowing a visual distinction of G-quadruplexes from other DNA conformations. Our results are of implications to biomedical studies, especially to high-throughput quadruplex-targeting anticancer drug screening. Further studies, especially computational simulations of the biosensing processes, are ongoing in our laboratories in an effort to better understand the binding modes of TTAPE with DNA molecules.

Experimental Section

General: Detailed information on materials, instrumentations, synthetic procedures, and characterization data for the dyes, data obtained from the supplementary and control experiments,

and selected crystal structures of a human telomeric DNA are given in the Supporting Information. DNA samples of G1, C1, and C2 were obtained from Operon in desalt purity and used without further purification. G1 was chosen as a model ssDNA molecule that mimics the human telomeric repeat sequence $d(T_2AG_3)$, which is capable of forming intramolecular G-quadruplex structures. Concentrations of the DNA strands were determined by measuring their absorptivity (ϵ) values at 260 nm in a 100- μ L quartz cuvette ($\epsilon \times 10^5 M^{-1} cm^{-1}$): 2.14 (G1), 1.85 (C1), 1.85 (C2)). Water was purified by a Millipore filtration system. Buffer solution was prepared by titrating 5 mM Tris with HCl until its pH value reached 7.50. All experiments were performed at room temperature unless otherwise specified.

PAGE assay: Electrophoresis assay of G1 was performed on a Hoefer miniVE system in $1 \times$ TBE buffer solution under nondenaturing conditions by using a 20% native poly(acrylamide) gel at 100 V for 3 h at 4°C. An AlphaDigiDoc system with a DE-500 MultiImage II light cabinet and an ML-26 UV transilluminator (Alpha Innotech) was used for data collection and analysis. The gel was poststained with a 10 μ M TTAPE solution for 5 min at room temperature, rinsed with distilled water, and photographed under UV light at 290–330 nm by the gel documentation system. EB was used to poststain the gel in parallel for comparison. Concentrations of G1 in the range of 0.5–10.0 μ M were used to check the ability of the dye-stained DNA in the PAGE assay to be visualized.

G-quadruplex formation: Complexes of ssDNA and TTAPE were prepared by mixing 10 μ L G1 (0.1 mM) and 50 μ L TTAPE (0.01 mM) in 5 mM Tris-HCl buffer solution in a 1.5-mL Eppendorf cup. The solution was in-

cubated at 4°C for 30 min. G-quadruplex formation was induced by adding 10 µL of a 1.0 M KCl solution into the Eppendorf cup. The final concentrations of TTAPE and G1 were kept at 4.5 and 9.0 µM, respectively. For other cationic species, the same amounts of corresponding salts were used. Kinetic experiments were conducted immediately after the injection of the cationic solution whereas other spectral measurements were performed after an incubation period of 30 min.

ITC measurement: Calorimetric titration experiments were performed at (25.00 ± 0.01) °C on a MicroCal VP-ITC apparatus. G1 solutions for the ITC experiments were prepared in all-potassium (K-Tris: 5 mM Tris-HCl and 150 mM KCl) or all-sodium (Na-Tris: 5 mM Tris-HCl and 150 mM NaCl) buffer solutions at pH 7.50, as required. The buffer solution of G1 was heated to 85°C and cooled slowly to ensure the folding of the DNA molecules into a G-quadruplex structures. For a typical titration, a series of 10 µL aliquots of TTAPE solution were injected into the G1/M⁺ solution at a 240 s interval. The heat for each injection was determined by the integration of the peak area in the thermogram with respect to time. Blank titration was conducted by injecting TTAPE into the sample cell containing only buffer solution under the same conditions. The interaction heat was corrected by subtracting the blank heat from that for the TTAPE/G1 titration. The *K_b* values were derived by fitting the isotherm curves with Origin 5.0 software.

Strand hybridization: Equimolar amounts of G1 and C1 were mixed in sterilized water. The solution was annealed at a temperature 2°C below *T_m* for 15 min, followed by a slow cooling to 25°C to allow double-helix formation. The procedures for the G quadruplex and C2 were carried out in the same manner.

FL kinetics: Time-dependent FL was measured on a FluostarOptima multifunctional microplate reader (BMG Labtechnologies) with $\lambda_{ex}/\lambda_{em}$ set at 350/470 nm. A solution of G1/TTAPE was transferred to a 96-well microtiter plate after incubation at 4°C for 30 min. Appropriate amounts of metal ions were added by an automatic injection mode. Kinetic measurements were performed at 20°C and the FL data were recorded every 4 s. The change in the emission intensity (*I*) of the solution after the addition of K⁺ can be fitted by a second-order exponential curve:^[9]

$$I = A_1 e^{-t/\tau_1} + A_2 e^{-t/\tau_2} + c \quad (1)$$

In Equation (1), *t* is the time, τ_1 and τ_2 are the time constants of FL recovery, *A*₁ and *A*₂ are the respective amplitudes (the folding process is characterized by negative *A* values), and *c* is the FL intensity at *t* = 8. Mean time constant (< τ >) was calculated according to Equation (2):

$$\tau = \frac{A_1 \tau_1 + A_2 \tau_2}{A_1 + A_2} \quad (2)$$

Acknowledgements

This project was partially supported by the Research Grants Council of Hong Kong (602707, 602706, HKU2/05C, and 603505), the Ministry of Science & Technology of China (2002CB613401), and the National Science Foundation of China (20634020). B.Z.T. thanks the support from Cao Guangbiao Foundation of Zhejiang University.

- [1] a) K. Collins, *Curr. Opin. Cell Biol.* **2000**, *12*, 378; b) R. K. Moyzis, J. M. Buckingham, L. S. Cram, M. Dani, L. L. Deaven, M. D. Jones, J. Meyne, R. L. Ratliff, J. R. Wu, *Proc. Natl. Acad. Sci. USA* **1988**, *85*, 6622; c) Y. Wang, D. J. Patel, *J. Mol. Biol.* **1993**, *234*, 1171.
 [2] a) J. T. Davis, *Angew. Chem.* **2004**, *116*, 684; *Angew. Chem. Int. Ed.* **2004**, *43*, 668; b) T. Simonsson, *Biol. Chem.* **2001**, *382*, 621; c) D. E. Gilbert, J. Feigon, *Curr. Opin. Struct. Biol.* **1999**, *9*, 305; d) R. H. Shafer, I. Smirnov, *Biopolymers* **2001**, *56*, 209.
 [3] a) J. A. Walmsley, J. F. Burnett, *Biochemistry* **1999**, *38*, 14063–14068; b) C. C. Hardin, *Biochemistry* **1991**, *30*, 4460; c) W. H. Braunlin, *Bio-*

- chemistry* **1993**, *32*, 13130; d) J. R. Williamson, M. K. Raghuraman, T. R. Cech, *Cell* **1989**, *59*, 871.
 [4] S. Borman, *C&E News* **2007**, *85*, 12.
 [5] a) M. Webba da Silva, *Chem. Eur. J.* **2007**, *13*, 9738; b) I. K. Moon, M. B. Jarstfer, *Front. Biosci.* **2007**, *12*, 4595; c) N. Maizels, *Nat. Struct. Mol. Biol.* **2006**, *13*, 1055.
 [6] a) A. De Cian, E. DeLemos, J. L. Mergny, M. P. T. Fichou, D. Monchaud, *J. Am. Chem. Soc.* **2007**, *129*, 1856; b) M. A. Blasco, *Nat. Rev. Genet.* **2005**, *6*, 611; c) R. T. Wheelhouse, D. Sun, H. Han, F. X. Han, L. H. Hurley, *J. Am. Chem. Soc.* **1998**, *120*, 3261.
 [7] a) J.-L. Mergny, J.-F. Riou, P. Mailliet, M.-P. Teulade-Fichou, E. Gilson, *Nucleic Acids Res.* **2002**, *30*, 839; b) G. Pennarun, C. Granotier, L. R. Gauthier, D. Gomez, F. Hoffschir, E. Mandine, J.-F. Riou, J.-L. Mergny, P. Mailliet, F. Boussin, *Oncogene* **2005**, *24*, 2917.
 [8] a) S. Neidle, G. Parkinson, *Nat. Rev. Drug Des.* **2002**, *1*, 383; b) A. T. Phan, V. Kuryavyi, J.-B. Ma, A. Faure, M.-L. Andréola, D. J. Patel, *Proc. Natl. Acad. Sci. USA* **2005**, *102*, 634.
 [9] a) G. N. Parkinson, M. P. H. Lee, S. Neidle, *Nature* **2002**, *417*, 876; b) J.-L. Mergny, J.-C. Maurizot, *ChemBioChem* **2001**, *2*, 124; c) H.-A. Ho, M. Leclerc, *J. Am. Chem. Soc.* **2004**, *126*, 1384–1387; d) Y. Zhao, Z. Y. Kan, Z. X. Zeng, Y. H. Hao, H. Chen, Z. Tan, *J. Am. Chem. Soc.* **2004**, *126*, 13255.
 [10] B. Juskowiak, *Curr. Anal. Chem.* **2006**, *2*, 261.
 [11] a) A. Bourdoncle, A. E. Torres, C. Gosse, L. Lacroix, P. Vekhoff, T. L. Saux, L. Jullien, J. L. Mergny, *J. Am. Chem. Soc.* **2006**, *128*, 11094; b) T. Simonsson, R. Sjöback, *J. Biol. Chem.* **1999**, *274*, 17379; c) F. He, Y. Tang, S. Wang, Y. Li, D. Zhu, *J. Am. Chem. Soc.* **2005**, *127*, 12343; d) W. Lv, N. Li, Y. Li, Y. Li, A. Xia, *J. Am. Chem. Soc.* **2006**, *128*, 10281.
 [12] E. E. Merkina, K. R. Fox, *Biophys. J.* **2005**, *89*, 365.
 [13] J. L. Mergny, *Biochemistry* **1999**, *38*, 1573.
 [14] a) J. Luo, Z. Xie, J. W. Y. Lam, L. Cheng, H. Chen, C. Qiu, H. S. Kwok, X. Zhan, Y. Liu, D. Zhu, B. Z. Tang, *Chem. Commun.* **2001**, 1740; b) J. Chen, C. C. W. Law, J. W. Y. Lam, Y. Dong, S. M. F. Lo, I. D. Williams, D. Zhu, B. Z. Tang, *Chem. Mater.* **2003**, *15*, 1535; c) J. Chen, B. Xu, X. Ouyang, B. Z. Tang, Y. Cao, *J. Phys. Chem. A* **2004**, *108*, 7522; d) H. Tong, Y. Dong, M. Haussler, J. W. Y. Lam, H. H. Y. Sung, I. D. Williams, J. Sun, B. Z. Tang, *Chem. Commun.* **2006**, 1133; e) Q. Zeng, Z. Li, Y. Dong, C. Di, A. Qin, Y. Hong, Z. Zhu, C. K. W. Jim, G. Yu, Q. Li, Z. Li, Y. Liu, J. Qin, B. Z. Tang, *Chem. Commun.* **2007**, 70; f) Y. Dong, J. W. Y. Lam, A. Qin, J. Sun, J. Liu, Z. Li, J. Sun, H. H. Y. Sung, I. D. Williams, H. S. Kwok, B. Z. Tang, *Chem. Commun.* **2007**, 3255.
 [15] For examples of TPE-based AIE dyes, see: a) H. Tong, Y. Hong, Y. Dong, M. Haussler, J. W. Y. Lam, Z. Li, Z. Guo, Z. Guo, B. Z. Tang, *Chem. Commun.* **2006**, 3705; b) H. Tong, Y. Hong, Y. Dong, M. Haussler, Z. Li, J. W. Y. Lam, Z. Li, Y. Dong, H. H. Y. Sung, I. D. Williams, B. Z. Tang, *J. Phys. Chem. B* **2007**, *111*, 11817; c) Y. Dong, J. W. Y. Lam, A. Qin, J. Liu, Z. Li, B. Z. Tang, *Appl. Phys. Lett.* **2007**, *91*, 011111.
 [16] a) B. K. An, S. K. Kwon, S. D. Jung, S. Y. Park, *J. Am. Chem. Soc.* **2002**, *124*, 14410; b) H. C. Yeh, S. J. Yeh, C. T. Chen, *Chem. Commun.* **2003**, 2632; c) S. Jayanty, T. P. Radhakrishnan, *Chem. Eur. J.* **2004**, *10*, 791; d) S. Li, L. He, F. Xiong, Y. Li, G. Yang, *J. Phys. Chem. B* **2004**, *108*, 10887; e) C. J. Bhongale, C. W. Chang, C. S. Lee, E. W. G. Diau, C. S. Hsu, *J. Phys. Chem. B* **2005**, *109*, 13472; f) S. J. Toal, K. A. Jones, D. Magde, W. C. Trogler, *J. Am. Chem. Soc.* **2005**, *127*, 11661; g) Z. Wang, H. Shao, J. Ye, L. Tang, P. Lu, *J. Phys. Chem. B* **2005**, *109*, 19627; h) Y. Sun, J. Liao, J. Fang, P. Chou, C. Shen, C. Hsu, L. Chen, *Org. Lett.* **2006**, *8*, 3713; i) M. R. Han, Y. Hirayama, M. Hara, *Chem. Mater.* **2006**, *18*, 2784; j) C. Bao, R. Lu, M. Jin, P. Xue, C. Tan, T. Xu, G. Liu, Y. Zhao, *Chem. Eur. J.* **2006**, *12*, 3287; k) Z. Xie, B. Yang, W. Xie, L. Liu, F. Shen, H. Wang, X. Yang, Z. Wang, Y. Li, M. Hanif, G. Yang, L. Ye, Y. Ma, *J. Phys. Chem. B* **2006**, *110*, 20993; l) Q. Peng, Y. Yi, Z. Shuai, J. Shao, *J. Am. Chem. Soc.* **2007**, *129*, 9333; m) C. Yuan, X. Tao, Y. Ren, Y. Li, J.-X. Yang, W. Yu, L. Wang, M. Jiang, *J. Phys. Chem. C* **2007**, *111*, 12811; n) Q. Zhao, L. Li, F. Li, N. Yu, Z. Liu, T. Yi, C. Huang, *Chem. Commun.* **2008**, 685.

- [17] a) H. Chen, J. W. Y. Lam, J. Luo, Y. Ho, B. Z. Tang, D. Zhu, M. Wong, H. S. Kwok, H. S. *Appl. Phys. Lett.* **2002**, *81*, 574; b) G. Yu, S. Yin, Y. Liu, J. Chen, X. Xu, X. Sun, D. Ma, X. Zhan, Q. Peng, Z. Shuai, B. Z. Tang, D. Zhu, W. Fang, Y. Luo, *J. Am. Chem. Soc.* **2005**, *127*, 6335.
- [18] J. E. McMurry, *Chem. Rev.* **1989**, *89*, 1513.
- [19] All absolute quantum yields (Φ_{Fa}) of AIE-active siloles are higher than their relative ones (Φ_{Fr}): for example, Φ_{Fa} of 1-methylpentaphenylsilole (85%) is fourfold higher than its Φ_{Fr} (21%).^[14a,17b]
- [20] Y. Q. Dong, J. W. Y. Lam, A. J. Qin, Z. Li, J. Z. Sun, H. H. Y. Sung, I. D. Williams, B. Z. Tang, *Chem. Commun.* **2007**, 40.
- [21] a) Furstenberg, T. G. Deligeorgiev, N. I. Gadjev, A. A. Vasilev, E. Vauthy, *Chem. Eur. J.* **2007**, *13*, 8600; b) A. Fuerstenberg, M. D. Julliard, T. G. Deligeorgiev, N. I. Gadjev, A. A. Vasilev, E. Vauthy, *J. Am. Chem. Soc.* **2006**, *128*, 7661; c) N. Svanvik, J. Nygren, G. Westman, M. Kubista, *J. Am. Chem. Soc.* **2001**, *123*, 803; d) J. Nygren, N. Svanvik, M. Kubista, *Biopolymers* **1998**, *46*, 39.
- [22] J. B. Birks, *Photophysics of Aromatic Molecules*, Wiley, London, **1970**.
- [23] a) C.-C. Chang, J.-Y. Wu, C.-W. Chien, W.-S. Wu, H. Liu, C.-C. Kang, L.-J. Yu, T.-C. Chang, *Anal. Chem.* **2003**, *75*, 6177; b) R. Westermeyer, *Electrophoresis in Practice: a Guide to Theory and Practice*, VCH, New York, **1993**.
- [24] a) S. Neidle, S. Balasubramanian, *Quadruplex Nucleic Acids*, RSC, London, **2006**, p. 26; b) P. Balagurumoorthy, S. K. Brahmachari, *J. Biol. Chem.* **1994**, *269*, 21858; c) H. Ueyama, M. Takagi, S. Takenaka, *J. Am. Chem. Soc.* **2002**, *124*, 14286; d) F. He, Y. Tang, M. Yu, F. Feng, L. An, H. Sun, S. Wang, Y. Li, D. Zhu, G. C. Bazan, *J. Am. Chem. Soc.* **2006**, *128*, 6764; e) J. Dai, C. Punchedhewa, A. Ambrus, D. Chen, R. A. Jones, D. Yang, *Nucleic Acids Res.* **2007**, *35*, 2440.
- [25] a) F. Rosu, V. Gabelica, K. Shin-ya, E. DePauw, *Chem. Commun.* **2003**, *34*, 2702; b) E. A. Venczel, D. Sen, *Biochemistry* **1993**, *32*, 6220.
- [26] A. Ambrus, D. Chen, J. Dai, T. Bialis, R. A. Jones, D. Yang, *Nucleic Acids Res.* **2006**, *34*, 2723.
- [27] I. Haq, J. O. Trent, B. Z. Chowdhry, T. C. Jenkins, *J. Am. Chem. Soc.* **1999**, *121*, 1768.
- [28] I. M. Dixon, F. Lopez, A. M. Tejera, J. P. Esteve, M. A. Blasco, G. Pratviel, B. Meunier, *J. Am. Chem. Soc.* **2007**, *129*, 1502?
- [29] J. J. Green, L. Ying, D. Klenerman, S. Balasubramanian, *J. Am. Chem. Soc.* **2003**, *125*, 3763.
- [30] C. C. Chang, C. W. Chien, Y. H. Lin, C. C. Kang, T. C. Chang, *Nucleic Acids Res.* **2007**, *35*, 2846, and references therein.
- [31] E. W. White, F. Tanius, M. A. Ismail, A. P. Reszka, S. Neidle, D. W. Boykin, W. D. Wilson, *Biophys. Chem.* **2007**, *126*, 140.

Received: November 1, 2007

Revised: April 11, 2008

Published online: June 2, 2008